Journal of Biomedical Optics

SPIEDigitalLibrary.org/jbo

Simultaneous optical coherence tomography and autofluorescence microscopy with a single light source

Cuixia Dai
Xiaojing Liu
Shuliang Jiao

Simultaneous optical coherence tomography and autofluorescence microscopy with a single light source

Cuixia Dai,[a] Xiaojing Liu,[b] and Shuliang Jiao[b]
[a]Shanghai Institute of Technology, College of Science, 100 Haiquan Road, Shanghai 201418, China
[b]University of Southern California, Department of Ophthalmology Keck School of Medicine, Los Angeles, California 90033

Abstract. We have accomplished simultaneous spectral domain optical coherence tomography (SD-OCT) and autofluorescence (AF) microscopy with a broadband light source centered at 415 nm. The light source was provided by frequency-doubling of an ultra-fast broadband Ti:Sapphire laser. With a bandwidth of 8 nm, the visible SD-OCT achieved a depth resolution of ~12 μm. Since the two imaging modalities are provided by the same group of photons, their images are intrinsically registered. The dual-modal system is capable of providing OCT imaging and molecular contrasts simultaneously. The imaging system was tested on imaging biological samples *ex vivo* and *in vivo*. [DOI: 10.1117/1.JBO.17.8.080502]

Keywords: dual-modality imaging; optical coherence tomography; autofluorescence microscopy.

Paper 12337L received May 31, 2012; revised manuscript received Jun. 27, 2012; accepted for publication Jun. 28, 2012; published online Jul. 13, 2012.

Optical coherence tomography (OCT)[1] and autofluorescence (AF) microscopy[2] are two optical imaging modalities that can image different yet complementary contrasts of biological tissues. OCT provides high-resolution, depth-resolved imaging mainly based on scattering contrast. AF imaging is based on fluorescence contrasts, which can provide maps of the distribution of endogenous molecules (fluorophores). In ophthalmic applications, OCT has been successfully used in clinical diagnosis for retinal diseases, while AF imaging has shown its advantages in early identification of the physiopathology of age-related macular degeneration (AMD) by detecting the accumulation of lipofuscin (LF) within the retinal pigment epithelium (RPE).[3]

Given their complimentary contrast mechanisms, the combination of OCT and AF imaging could potentially provide more sensitive and specific detection of disease than either modality alone. Several groups have investigated the combination of OCT with AF imaging and demonstrated the diagnostic capabilities of this combination by imaging pathological changes in different biological tissues.[4–11] In these studies, two different light sources at different wavelengths were used for OCT and fluorescence excitation. Accomplishing OCT and AF imaging with a single light source has not been demonstrated before. In ophthalmic diagnosis, the combination of OCT and AF imaging with a single light source may further facilitate the research and early diagnosis of retinal diseases by imaging both the optical scattering and molecular contrast at the same wavelengths.

In our previous studies we have developed a visible light OCT (VIS-OCT)with a broadband light source centered at 415 nm.[12] Since biomolecules like lipofuscin fluoresce when illuminated with light at this band, this system provides us an opportunity to achieve both OCT and AF imaging simultaneously. Such a dual modal imaging system can provide simultaneous depth-resolved scattering contrast by detecting the back-scattered light with an interferometer in the spectral domain and molecular contrast by detecting the AF signal emitted from fluorophores. Since the two imaging modes are generated from the same group of photons, their images are intrinsically registered.

Figure 1 shows a schematic of the experimental system. A broadband Ti: Sapphire laser (MICRA, center wavelength: 800 nm, bandwidth: 120 nm, Coherent Inc.) was used as the fundamental light source. The fundamental laser light was focused into a frequency doubling crystal (BBO, Castech, Fujian, China) by a lens of $f = 14$ mm (L1) and converted to the visible. The light exiting the BBO crystal (bandwidth ~8 nm) was first collimated with an achromatic lens of $f =$ 40 mm (L2) and then reflected by a long-pass filter (FEL0700, Thorlabs) to separate the visible light from the residual fundamental light. The visible light beam was coupled into the source arm of a single-mode optical fiber-based Michelson interferometer. After exiting the sample arm, the light was collimated, reflected by a dichroic mirror (NT69-887, cut on wavelength: 450 nm, Edmund Optics, Inc.), scanned by an $X - Y$ galvanometer scanner, and then focused on the sample by an achromatic lens (L3, $f = 75$ mm). When imaging the retina *in vivo* an objective lens (L4, $f = 19$ mm) was added. In the detection arm, the reflected light from the sample and reference arms was collimated and detected by a spectrometer, which consisted of an 1800 line/mm transmission grating, a multi-element imaging lens ($f = 150$ mm), and a line scan CCD camera (Aviiva-SM2-CL-2010, 2048 pixels with 10 μm pixel size operating in 12-bit mode, e2V). An image acquisition board (NI IMAQ PCI 1428) acquired the image captured by the camera and transferred it to a workstation (HP xw4600, 4 GB memory) for signal processing and image display.

The back-traveling fluorescent photons emitted from the sample passed through the dichroic mirror and a long-pass filter (FEL0450, cut on wavelength: 450 nm, Thorlabs, Inc.), and was then focused into a 20-μm pinhole by a lens of $f = 30$ mm (L5).The AF photons were detected by a photomultiplier module (PMM02, Thorlabs, Inc.). The AF signals were digitized by a multifunction data acquisition board (DAQ, NI PCIe-6361, National Instruments) at a sampling rate of 1 MS/s.

Synchronization of the AF data acquisition, scanning of the galvanometer scanner and the OCT data acquisition was controlled by the multifunction DAQ board. The linear CCD camera in the OCT spectrometer was operated at a line rate of 12k lines per second, and the integration time was set to 70 μs. Similar to

Address all correspondence to: Shuliang Jiao, University of Southern California, Department of Ophthalmology, Keck School of Medicine, 1450 San Pablo St., Room DVRC 307E Los Angeles, California 90033; E-mail: sjiao@usc.edu.

0091-3286/2012/$25.00 © 2012 SPIE

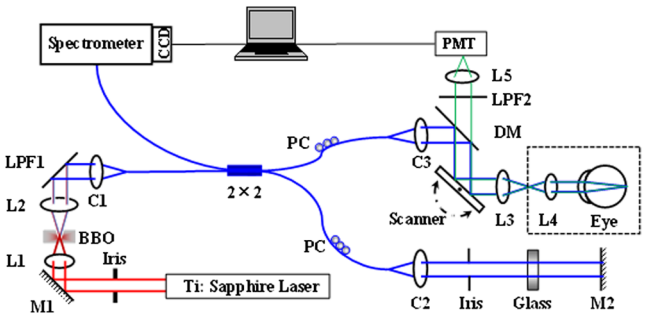

Fig. 1 Schematic of the dual-modal OCT and AF imaging system. The dashed box represents the parts used for *in vivo* retinal imaging. M1-M2: Mirror; C1-C3: Collimator; L1-L5: Lens; BBO: BBO crystal; DM: Dichroic mirror; LPF1- LPF2, Long-pass filter; PC: Polarization controller; PMT: Photomultiplier.

that reported in our previous publications, the VIS-OCT has a depth resolution of ~12 μm and an imaging depth of 1.3 mm in the air.

To test the capability of the dual-modal imaging technique, we first imaged the ciliary body of an excised pig eye. The eye was acquired from a local slaughter house and was preserved in 10% formalin solution. The light power in front of the sample was about 525 μW. The lateral resolution was calculated to be about 15.9 μm.

Figure 2 shows the simultaneously acquired OCT [Fig. 2(a) and 2(b)] and AF images [Fig. 2(c)] of the ciliary body. Figure 2(a) shows the projection of the three-dimensional (3-D) OCT dataset. The images cover an area of 1.5×1.5 mm^2 consisting of 512 (horizontal) ×128 (vertical) pixels. From Fig. 2(a) and 2(c), we can see that regions giving higher OCT signal also give higher AF signal. From our previous experiments by using multimodal photoacoustic microscopy, we know that the dark areas in the AF image are melanin granules.[13] The OCT projection image clearly shows the competition of two physical processes: optical scattering and optical absorption. We can see that in melanin optical absorption is much more significant than optical scattering at the probing wavelength. The absorbed photons were mainly converted to heat. Yet in areas surrounding the melanin granules, the probing light was both scattered and absorbed. The scattered photons contributed to the OCT signal while the absorbed photons were reemitted as AF. Due to the high scattering and absorption coefficients of the tissue, the penetration depth of the probing light is very limited.

Our goal for this dual modal imaging technique is to image the retina. To test the feasibility the system was applied to imaging the normal rat retina *in vivo*. The animal (Sprague Dawley rat, body weight: 450 g, Charles Rivers) was anesthetized by intraperitoneal injection of a cocktail containing ketamine (54 mg/kg body weight) and xylazine (6 mg/kg body weight). The pupil was dilated with 10% phenylephrine solution. Drops of artificial tears were applied to the eyes every 2 min to prevent dehydration of the cornea and cataract formation. After anesthetization, the animals were restrained in a mounting tube, which was fixed on a five-axis platform. The light power in front of the eye was about 405 μW, which is below the ANSI safety limits for eye imaging.

Figure 3 shows the simultaneously acquired OCT [Fig. 3(a) and 3(b)] and AF [Fig. 3(c)] images of the rat retina. Figure 3(a) is a projection of the 3-D OCT dataset (OCT fundus image). As shown in Fig. 3(b), the blood vessels block the probing light completely with only reflections from their front boundaries. The retinal blood vessels appear dark in both the OCT fundus and AF images as a result of high optical absorption of hemoglobin in the probing wavelengths. Due to the dark appearance of the vessels in the AF image, we can also conclude that the AF signals are generated in tissues behind the retinal vessels. We believe that the AF signals are mainly contributed from lipofuscin in the RPE cells. As a result, the AF image represents lipofuscin distribution in the RPE layer.

In conclusion, we have for the first time achieved simultaneous OCT and AF imaging with a single broadband light source, which can provide both structural and molecular imaging of biological tissues. The acquired OCT and AF images are intrinsically registered. We have successfully imaged *ex vivo* ocular tissues and the rat retina *in vivo*. Since many biomolecules fluoresce when stimulated at around 415 nm, the application of the current system is limited. When a broadband light source centered at other wavelengths, e.g., 500 nm, is used, the system will be potentially useful for imaging the structure

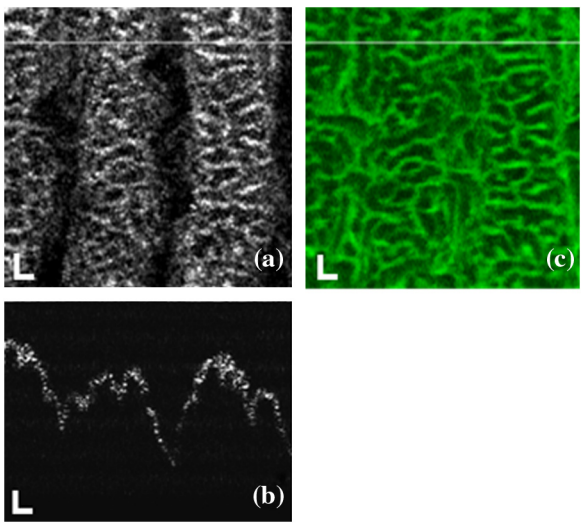

Fig. 2 VIS-OCT and AF images simultaneously acquired from the ciliary body of an excised pig eye: (a) OCT projection image; (b) VIS-OCT B scan image; (c) AF image. Bar: 100 μm.The white line in the OCT projection image marked the location of the VIS-OCT B-scan image.

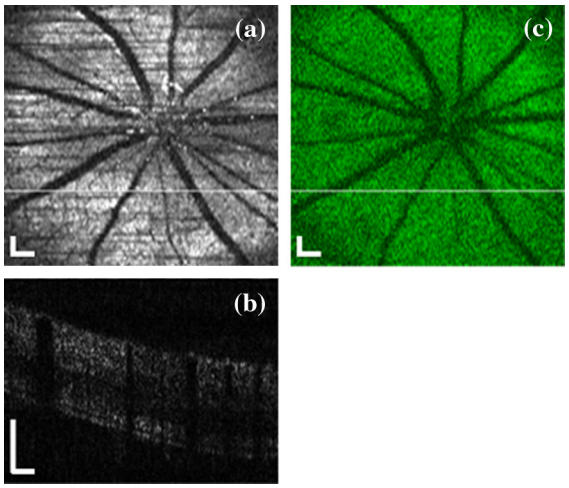

Fig. 3 VIS-OCT and AF images simultaneously acquired from the rat retina. (a) OCT fundus image; (b)VIS-OCT B-scan image; (c) AF image. Bar: 200 μm. The white line in the OCT fundus image marked the location of the VIS-OCT B-scan image.

and lipofuscin of the RPE layer.[13] Since the OCT and AF signals come from the same group of photons, the two imaging modalities are correlated. Our ultimate goal is to achieve depth-resolved AF imaging by combining OCT images in both the visible and near-infrared bands. The current work is just a proof of concept, which has been proved to be successful.

Acknowledgments

This work is supported in part by the following grants: National Institutes of Health Grant 1R01EY019951-01A1 and Coulter Translational Award.

References

1. D. Huang et al., "Optical coherence tomography," *Science* **254**(5035), 1178–1181 (1991).
2. N. Ramanujam, "Fluorescence spectroscopy of neoplastic and non-neoplastic tissues," *Neoplasia* **2**(1–2), 89–117 (2000).
3. D. C. Gray et al., "In vivo fluorescence imaging of primate retinal ganglion cells and retinal pigment epithelial cells," *Opt. Express* **14**(16), 7144–7158 (2006).
4. R. V. Kuranov et al., "Combined application of optical methods to increase the information content of optical coherent tomography in diagnostics of neoplastic processes," *Quantum Electron.* **32**(11), 993–998 (2002).
5. L. P. Hariri et al., "Endoscopic optical coherence tomography and laser-induced fluorescence spectroscopy in a murine colon cancer model," *Lasers Surg. Med.* **38**(4), 305–313 (2006).
6. Z. G. Wang et al., "Fluorescence guided optical coherence tomography for the diagnosis of early bladder cancer in a rat model," *J. Urol.* **174**(6), 2376–2381 (2005).
7. A. Bradu et al., "Dual optical coherence tomography/fluorescence microscopy for monitoring of Drosophila melanogaster larval heart," *J. Biophoton.* **2**(6–7), 380–388 (2009).
8. J. Park et al., "A dual-modality optical coherence tomography and fluorescence lifetime imaging microscopy system for simultaneous morphological and biochemical tissue characterization," *J. Biomed. Opt.* **1**(1), 186–200 (2010).
9. S. Yuan et al., "Co-registered optical coherence tomography and fluorescence molecular imaging for simultaneous morphological and molecular imaging," *Phys. Med. Biol.* **55**(1), 191–206(2010).
10. N. Iftimia et al., "Fluorescence-guided optical coherence tomography imaging for colon cancer screening: a preliminary mouse study," *Biomed. Opt.Express* **3**(1), 178–191(2012).
11. A. D. Singh et al., "Fourier domain optical coherence tomographic and auto-fluorescence findings in indeterminate choroidal melanocytic lesions," *Br. J. Ophthalmol.* **94**(4), 474–478 (2010).
12. X. Y. Zhang et al., "Dual-band spectral-domain optical coherence tomography for *in vivo* imaging the spectral contrasts of the retinal nerve fiber layer," *Opt. Express* **19**(20), 19653–19659 (2011).
13. X. Y. Zhang et al., "Simultaneous *in vivo* imaging of melanin and lipofuscin in the retina with photoacoustic ophthalmoscopy and autofluorescence imaging," *J. Biomed. Opt.* **16**(8), 080504 (2011).